

Nuclear Fusion in Laser-Driven Counter-Streaming Collisionless Plasmas

Xiaopeng Zhang,¹ Jiarui Zhao,² Dawei Yuan,³ Changbo Fu,^{1,*} Jie Bao,⁴ Liming Chen,^{2,5} Jianjun He,^{3,6} Long Hou,⁴ Liang Li,¹ Yanfei Li,² Yutong Li,^{2,5,†} Guoqian Liao,² Yongjoo Rhee,⁷ Yang Sun,^{1,5} Shiwei Xu,⁶ Gang Zhao,³ Baojun Zhu,² Jianqiang Zhu,⁸ Zhe Zhang,² and Jie Zhang^{1,5}

¹*Department of Physics and Astronomy, Shanghai Jiao Tong University, Shanghai, 200240, China*

²*Laboratory of Optical Physics, Institute of Physics, Chinese Academy of Sciences, Beijing 100190, China*

³*National Astronomical Observatories, Chinese Academy of Sciences, Beijing 100012, China*

⁴*Department of Nuclear Physics, China Institute of Atomic Energy, Beijing, 102413, China*

⁵*IFSA Collaborative Innovation Center, Shanghai Jiao Tong University, Shanghai 200240, China*

⁶*Institute of Modern Physics, Chinese Academy of Sciences, Lanzhou, 730000, China*

⁷*Center for Relativistic Laser Science, IBS, Gwangju 61005, Korea*

⁸*Shanghai Institute of Optics and Fine Mechanics, Chinese Academy of Sciences, Shanghai 201800, China*

(Dated: May 24, 2022)

Nuclear fusion reactions are the most important processes in nature to power stars and produce new elements, and lie at the center of the understanding of nucleosynthesis in the universe. It is critically important to study the reactions in full plasma environments that are close to true astrophysical conditions. By using laser-driven counter-streaming collisionless plasmas, we studied the fusion $D+D \rightarrow n+{}^3\text{He}$ in a Gamow-like window around 27 keV. The results show that astrophysical nuclear reaction yield can be modulated significantly by the self-generated electromagnetic fields and the collective motion of the plasma. This plasma-version mini-collider may provide a novel tool for studies of astrophysics-interested nuclear reactions in plasma with tunable energies in earth-based laboratories.

Collisionless plasma (CLP) exists in many astrophysical environments. Well-known examples of CLPs are widely-found collisionless shockwaves in supernovae remnants, in gamma-ray bursts, and in solar winds, etc[1]. In these special environments, nucleosynthesis cross sections could be significantly different from that in usual cases due to the following facts. Firstly, the energy distribution of the particles in a CLP may be far from thermal equilibrium. Due to the “collisionless” features[2], some charged particles in it can be continuously accelerated in a large scale without losing their energy too much through scattering [3], and the system can keep in non-thermal equilibrium for long time. Secondly, the self-generated macro-scale electromagnetic field, originating from the effects such as the Biermann battery effect and the Weibel instability [4], can affect the motion of the particles, and thus their nuclear reaction yield. Lastly, the reaction yield could be significantly modified by the so-called electron screening effect [5]. For nuclei in the normal atomically-bound states, their decay properties and reaction rates can be completely different from those in plasma environments [6, 7]. However, almost all nuclear parameters used as astrophysical inputs are traditionally measured under non-plasma environments. Obviously, creation of plasma conditions in terrestrial laboratories for studying astrophysical nuclear reactions is critically important, which may help solving some long-standing nucleosynthesis puzzles, as for instance, the puzzles on ${}^{26}\text{Al}$ [8] and ${}^{6,7}\text{Li}$ abundance [9].

The development of high-intensity laser technologies makes it possible to create plasma environments for nuclear studies in earth-based laboratories [10], for example, the coulomb explosion method [11, 12], the inertial con-

fining fusion method [13], and the double lasers method [14] etc. However, these methods have limits like untunable energy, large facility needed etc.

Here we report the studies of $D(d,n){}^3\text{He}$ in a CLP by using laser-driven head-on-head collision of plasma streams[15–21]. Because of the head-on-head collision, there is an enhancement of the center-of-mass (c.m.) energy by a factor of four. The reaction yields are thereby significantly enhanced as the reaction cross-section increases exponentially with the c.m. energy. We show that this kind of mini-version plasma collider [22] could be an ideal method for studying nuclear reactions in plasmas at earth-based laboratories with features like tunable energies to cover the astrophysical Gamow window [5].

The experiment was carried out at the Shenguang II laser facility, the National Laboratory on High Power Lasers and Physics in Shanghai, China. The experimental setup is shown in Fig.1. There were eight laser beams at this facility, each of which could deliver an energy of about 250 J with the pulse width of 1 ns at wavelength of 351 nm (3ω). Two targets were located at the center of the laser chamber. Both of the targets had $0.5 \times 0.5 \text{ mm}^2$ sized copper bases which were coated with 5 or 10 μm thick deuterated hydrocarbon ($\text{CD}_{1.29}$) layers and a separation of 4.4 mm between them [23]. The main lasers were arranged as two sets (4+4) and each set had four lasers focusing on one of the targets. The diameter of the focus spots was about 150 μm , producing a laser intensity of about $6 \times 10^{15} \text{ W/cm}^2$.

Another laser with a duration of 70 ps and wavelength of 526 nm was used as the probe, which passed through the plasma generated by the main laser beams. The interference images were taken by a Nomarski interferome-

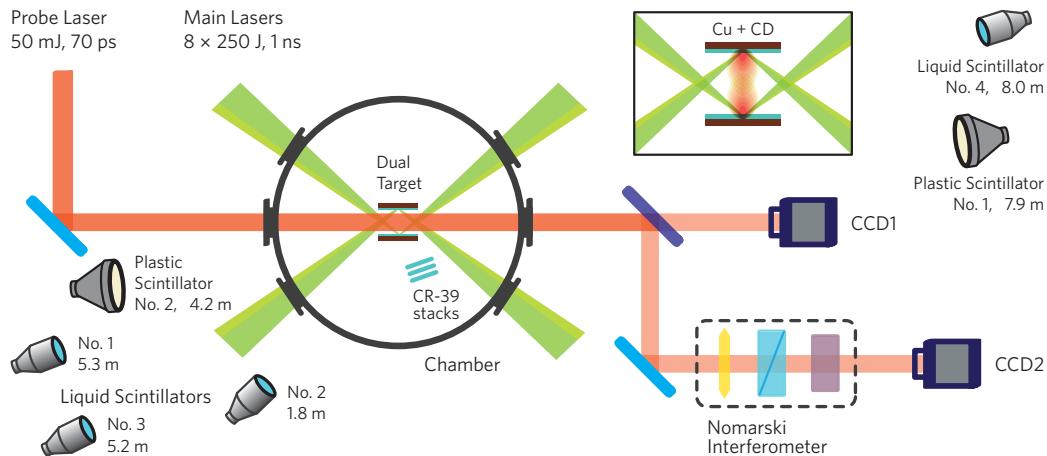


FIG. 1: The experimental setup. Four laser beams were tuned to focused on the target at one side, and another 4 on the opposite side. By using the probe laser and a Nomarski interferometer, the optical images of the plasma were taken. Neutron signals were recorded by scintillation detectors at different distances.

ter [24, 25]. By tuning the delay time between the probe laser and the main lasers, snapshots of the plasma at different times could be taken.

Neutron detectors were located outside the laser target chamber. Four of the them were liquid scintillation detectors (EJ-301) with scintillator size of $(\pi/4) \times 12.7^2 \times 12.7$ cm³, along with two plastic detectors (BC400) with scintillator size of $(\pi/4) \times 25.4^2 \times 5$ cm³. All scintillators were directly coupled with photomultiplier tubes (PMTs). The signals were recorded by oscilloscopes with a bandwidth of 1 GHz. The neutrons were measured by the time-of-flight (TOF) approach.

Typical TOF spectra are shown in Fig. 2, in which the results from four liquid scintillation detectors at different locations are given. In each of the curves, the first dip to the left, which saturates the detectors, represents the photons induced by the high-intensity lasers. The photons, including X-rays and γ -rays, are induced by the original 351 nm, 1 ns width laser pulse and scattered secondary photons on the materials around the targets. Since most X-ray and γ -ray emissions in atoms or nuclei are in a smaller-than 1 ns domain, they are expected to arrive at the detectors as a ns-width pulse, which is the same pulse width as the original driving laser. Within such a narrow width, the photons are highly overlapped, and some detectors may be saturated. The long tail of the first dip is due to the long discharging time of the PMTs.

The second dip in the curves in Fig. 2 represents the neutron products. The neutrons from the $D(d,n)^3\text{He}$ reaction have an energy of $E_n = 2.45$ MeV, or an speed of 2.16 cm/ns, which is much smaller than that of the photons (30 cm/ns). The expected neutron speed and the measured neutron speeds at different detector locations

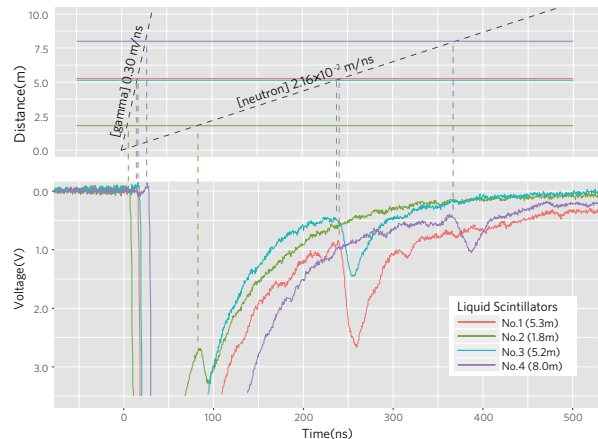


FIG. 2: Typical time-of-flight (TOF) spectra of neutron detectors. Data from the four liquid scintillation detectors at distance 1.8 m, 5.2 m, 5.3m, and 8.0 m, are shown. The expected arriving time of photons and neutrons (2.45 MeV) for each detector are indicated by dashed lines. They match well with the TOFs measured by detectors at different distances.

show good agreement with each other.

To obtain absolute neutron yields, all detectors have been calibrated by using two radiation sources, a D-D neutron generator and a ¹³⁷Cs γ -ray source. The Monte Carlo (MC) simulation code, GEANT4 [26], is employed for the calibration. In the MC simulation, after the to-be-detected particles depositing energies in the scintillator, the energy is transferred to luminescent photons with different efficiencies for neutrons and γ -ray [27].

The final neutron yields for different runs are obtained by combining the MC simulation, the experimental calibration data of the ¹³⁷Cs γ source and the neutron generator, as well as weighted values of all detectors. The

results are shown in Tab. I.

In the experiment, the observed neutrons might come from three sources: from the original laser-induced fireballs (N_{fb}), from the cold target when the energetic deuterium ions from the opposite target hit it (N_{cold}), and from the area where two plasma currents collide with each other ($N_{collide}$). The total neutron yield is the sum of all the three sources, i.e. $N_{total} = N_{fb} + N_{cold} + N_{collide}$.

To see how many neutrons come from the original fireballs, we either took off the second CD target (Tab. I, Run35), or left only a target base there but without CD film on it (Tab. I, Run38–40), while keeping all other laser parameters the same. The results have shown no evidence of neutrons from those runs, i.e. under the detecting limit of $< 2 \times 10^3$ (95% C.L.).

To determine N_{cold} , four lasers were focused on one of the two CD targets, but no laser directly focused on the opposite one. The neutron yields for this setup was 0.5×10^5 (Tab. I, Run80 and 81), which was much smaller than the cases with double targets. It should be pointed out that the second target was not totally “cold”. Since this target was only 4.4 mm away from the opposite one, it could also be ionized by the scattered laser and the X-ray coming from the opposite target [28]. In fact, plasma on the opposite target surface was observed on the interferometer images in these runs.

Comparing the measured N_{fb} , N_{cold} , and $N_{collider}$, one can conclude that the neutron yields are dominated by ion collisions, and the present setup provides an efficient way to ignite nuclear fusion reactions in a mini-size collider.

The Abel inversion approach has been employed to deduce the electron density n_e . Since the spatial distribution of the plasma is not ideally symmetrical, we followed a numerical method for asymmetrical Abel inversion described in Ref. [29].

For the CD_{1,29} targets used in the experiment, considering the charge neutrality of plasma in the μm scale and the fact that the carbon and deuterium atoms were fully ionized in the energy range of interest (> 5 keV), the density of deuterons in the plasma can be estimated as

$$n_D \approx \frac{1.29}{6 + 1.29} n_e. \quad (1)$$

The deuteron density estimated in this way has been confirmed by the MULTI2D hydrodynamics code [30].

A typical density distribution is shown in Fig. 3. From the data, one can estimate the collision frequency between electrons (e-e), electrons and deuteron ions (e-D), and D-D. The D-D mean free path, λ_{DD} , can be written as [31]:

$$\lambda_{DD} = \frac{m_D^2 v_{12}^4}{4\pi Z^4 e^4 n_D \ln \Lambda_{12}}, \quad (2)$$

where m_D is the deuteron mass, v_{12} the relative velocity, Ze the ion’s charge, and $\ln \Lambda_{12}$ the so-called “Coulomb

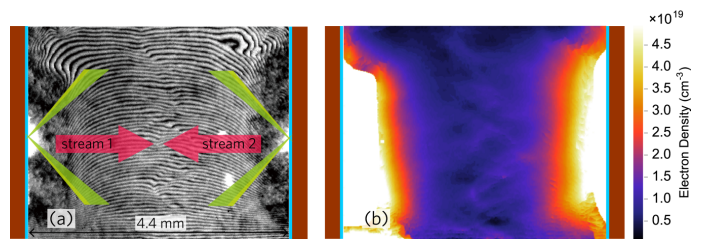


FIG. 3: (a) A typical Nomarski interferogram of the plasma streams, and (b) the corresponding electron density distribution derived by Abel inversion approach.

logarithm” [32]. With our experimental setup, in the relative velocity range $v_{12} > 1 \times 10^8$ cm/s, (corresponding to $E_{cm} > 5.2$ keV), λ_{DD} is calculated to be larger than 46 mm, which is much larger than the separation between the two targets (4.4 mm). Therefore the plasma is really “collisionless” for deuteron energy larger than 5.2 keV. The e-D collision frequency of 3×10^{10} /s can also be estimated. This means that the electrons could collide with other electrons and ions for about 30 times in 1 ns. Consequently, a quasi thermal equilibrium of ions is established.

A numerical calculation has been carried out with a simplified plasma dynamic model to obtain the expected neutron yields. Considering the fact that N_{fb} is very small, we assume that the deuterons from one target can only have reactions with those from the opposite side, and the D-D neutrons from the same side are negligible. The reaction yield can be written as [5],

$$Y = \iiint n_{1D}(\vec{r}_1) n_{2D}(\vec{r}_2) \sigma(v_1, v_2) d\vec{r}_1 d\vec{r}_2 dS, \quad (3)$$

where n_{1D} and n_{2D} are the deuteron densities of the left and right sides, respectively. The cross section is

$$\sigma(E_{cm}) = S(E_{cm}) \exp(-2\pi\eta)/E_{cm}, \quad (4)$$

where $E_{cm} = \frac{m}{4}(v_1 + v_2)^2$ is the center-of-mass energy (c.m.e.), $S(E_{cm})$ defined by this equation is the so-called astrophysical S-factor, and $\eta = \frac{Z_1 Z_2 e^2}{\hbar(v_1 + v_2)}$ is the Sommerfeld parameter.

We have simplified the ion speed v as a constant in the collisionless regime, i.e. $v = z/t_0$, where t_0 is the delayed time of the probe laser, and z is the distance to the target. n_D is separated into left part and right part which are originally from the left and right targets, i.e. $n_D = n_{1D} + n_{2D}$.

Figure 4 shows the D-D reaction yield for different velocities in plasma with the assumptions described above. One can find that the $N_{ion}(E_{cm})$, the number of ion pairs with c.m.e. E_{cm} , decreases as E_{cm} increases; while the $\sigma(E_{cm})$ increases as E_{cm} increases. Therefore, according to Eq. 3, large reaction yields are found in the c.m.e. range of 15 to 40 keV, as shown in Fig. 4(a).

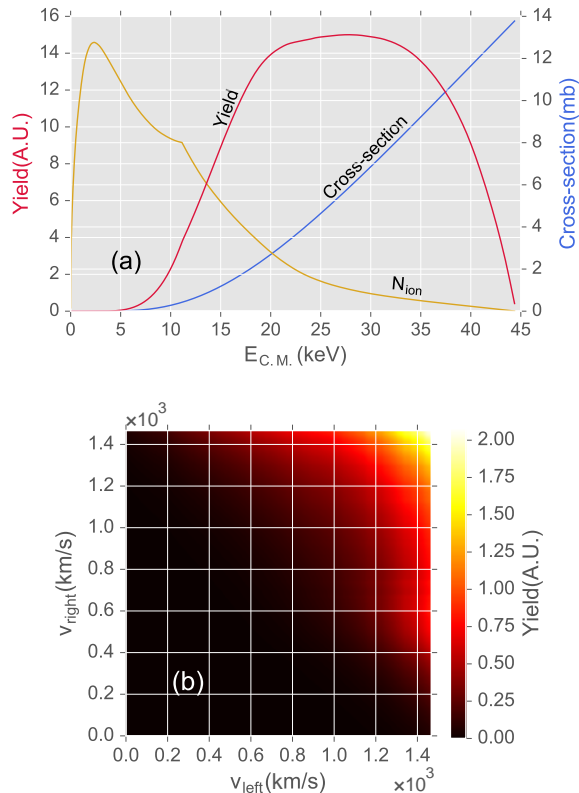


FIG. 4: Neutron yields contributed by deuterium ions with different c.m. energies. (a) the Gamow-window-like feature of the reaction yield. Three lines are shown in this chart: the number of the ions, the D(d,n)³He cross section, and the neutron yield. (b) The neutron yield generated by ion pairs with different speed. The x-axis is the speed of the ions from the left target (V_{left}), and the y-axis, the right target (V_{right}).

This Gamow-window-like [5] structure implies that the present method could be a promising new tool for the key reactions with nuclear-astrophysical interest, which are otherwise very difficult, if not impossible, to preform in traditional experimental setups.

The calculated neutron yield by using the simplified model is $(3.1 \pm 1.2) \times 10^6$ for Run37, or 8 times larger than the experimental observation. This disagreement may be due to the neglected self-generated magnetic fields in our calculation. With the current experimental conditions, the head-on-head collision of plasma streams can generate a toroidal field inversely proportional to electron density and the distance to the symmetrical axis, i.e. $B_\phi/n_{er} = \text{const}$ [33]. This type of fields has been reported in previous experiments with the similar head-on-head collision setup [21, 34], and the magnetic field strength is estimated to be about 10 T level. Under this field strength, the deuterons with an energy of tens keV can be significantly bent from a straight path. Therefore the c.m.e. of the ion pairs should become smaller, thus resulting a smaller neutron yield.

The method introduced in this article could have far-reaching implications for future nuclear reaction experiments aiming at understanding of the origin of element production in the universe.

First, this method provides a controllable way to trigger nuclear reactions within the Gamow window [5]. Nuclear astrophysical interested reactions are normally have very small cross sections, and traditional accelerators have very low peak beam intensities, which result in the very low signal to background noise ratio. Therefore, it is very difficult to study nuclear reactions in their Gamow windows with traditional accelerators. Compared with the coulomb explosion method [11], whose energy is hardly tunable, the current setup is likely the only known controllable method which can provide particles with quasi-Boltzmann distribution for nuclear astrophysical studies up to date.

Second, this setup provides a lab-based full plasma environment for nuclear reactions studies. There have been strong indications that the decay properties and reaction rates of bare nuclei in plasmas differ significantly from those of atomically-bound states obtained from normal conditions[6, 7]. Compared with other methods, for example the Coulomb explosion method [11] or the storage ring method [35], the plasma in this work is charge neutral, and the environment created here is more similar as that in real astrophysical cases.

Third, the results show hints that the self-generated macro-scale electromagnetic field may play an important role in the nucleosynthesis of our universe. A plasma in a “collision” state means that ions in it collide with each other frequently, so that the system can quickly reach a thermal equilibrium; while a “collisionless” state means that the ions rarely collide and the system is far from a thermal equilibrium. Because of the collisionless features, the nuclei inside CLPs can process in macro-scale lengths before being scattered, and thus acquire energy due to the self-generated macro-scale electrical field [18]. This can accelerate the nuclei and/or change their paths, and therefore the reaction yields could be completely different from that in thermal equilibriums, as observed in the present experiment. More nuclear reaction studies in a laboratory CLP may an important step toward solving the long-standing puzzles like the ^{6,7}Li abundance in Big Bang Nucleosynthesis [9].

In summary, we have presented a novel experimental method for studying nuclear reactions in plasma environments. Taking advantages of the extremely-high peak of ion flux and high temperature induced by lasers, stellar environments could be simulated, in which low energy and small cross section nuclear reactions could be studied on earth-based laboratories. By employing this method, the D(d,n)³He reaction has been performed by using head-on-head collision of plasma streams driven by nanosecond pulse lasers. The experimental results have shown that the neutron yield from the nuclear reaction

TABLE I: The neutron yields at different runs. (See the text for details)

Run#	Lasers ^a	Laser Energy(J)	Target1	Target2	Neutron yield
34	4+4	297×8	CD(10μm)	CD(10μm)	$(3.8 \pm 1.1) \times 10^5$
35	4+0	260×4	CD(10μm)	-	0
36	4+4	254×8	CD(10μm)	CD(10μm)	$(4.0 \pm 1.2) \times 10^5$
37	4+4	244×8	CD(10μm)	CD(10μm)	$(3.9 \pm 1.1) \times 10^5$
38	4+4	254×8	CD(10μm)	Cu(only)	0
39	4+4	217×8	CD(10μm)	Cu(only)	0
40	4+4	246×8	CD(10μm)	Cu(only)	0
79	4+4	230×8	CD(10μm)	CD(10μm)	$(1.0 \pm 0.5) \times 10^5$
80	4+0	263×4	CD(10μm)	CD(10μm)	$(0.5 \pm 0.3) \times 10^5$
81	4+0	219×4	CD(10μm)	CD(10μm)	$(0.6 \pm 0.3) \times 10^5$

^a“ $M + N$ ” means: M lasers focused on the first target, and N lasers on the second one. See the text for details.

are enhanced significantly by the head-on-head collision in the CLPs. And we have found evidences that the self-generated electromagnetic fields in CLPs might affect the nuclear reaction yield significantly. This novel plasma-version mini-collider can be employed in future studies of nuclear astrophysical processes, the magnetic confinement fusion, and possibly more others.

We would like to acknowledge the SG-II staff for operating the laser facility, CAEP staff for the target fabrication. This work is supported by the National Basic Research Program of China (Grant Nos. 2013CBA01501, 2013CB834401), the National Nature Science Foundation of China (Grant Nos. 11135012, 11135005, 11375114), and the Global R&D Networking Program funded by the Republic of Korea’s Ministry of Science, ICT and Future Planning (Grant No. NRF-2012-0004839). One of us (CBF) thanks for the supports from Shanghai Municipal Science and Technology Commission (under grant No. 11DZ2260700), the Key Lab for Particle Physics, Astrophysics and Cosmology, Ministry of Education, and Shanghai Key Lab for Particle Physics and Cosmology(SKLPPC).

* Corresponding author:cbfu@sjtu.edu.cn

† Corresponding author:ytli@iphy.ac.cn

[1] D. Biskamp, Nuclear Fusion **13**, 719 (1973).

[2] A. Bret, J. Plasma Phys. **81**, 455810202 (2015).

[3] R. Blandford and D. Eichler, Physics Reports **154**, 1 (1987).

[4] D. Ryu *et al.*, Sp. Sci. Rev. **166**, 1 (2012).

[5] C. E. Rolfs and W. S. Rodney, *Cauldrons in the cosmos* (University of Chicago press, 1988).

[6] Y. A. Litvinov and F. Bosch, Reports on Progress in Physics **74**, 016301 (2013).

[7] K. Czernski, A. Huke, A. Biller, P. H. abd M. Hoefft, and G. Ruprecht, Europhys. Lett. **54**, 449 (2001).

[8] N. Prantzos and R. Diehl, Phys. Rep. **267**, 1 (1996).

[9] R. H. Cyburt *et al.*, Rev. of Mod. Phys. **88**, 015004 (2016).

[10] B. Remington, Science **284**, 1488 (1999).

[11] T. Ditmire *et al.*, Nature **398**, 489 (1999).

[12] M. Barbui, W. Bang, A. Bonasera, *et al.*, Phys. Rev. Lett. **111**, 082502 (2013).

[13] Y. Kim *et al.*, Phys. Plasmas **19**, 056313 (2012).

[14] C. Labaune *et al.*, Nat. Comm. **4** (2013).

[15] C. Li, D. Ryutov, S. Hu, *et al.*, Phys. rev. Lett. **111**, 235003 (2013).

[16] Y. Kuramitsu *et al.*, Astro. phys. J Lett. **707**, L137 (2009).

[17] D. D. Ryutov *et al.*, Phys. of Plasmas **18**, 104504 (2011).

[18] N. L. Kugland *et al.*, Nat. Phys. **8**, 809 (2012).

[19] J. Ross *et al.*, Phys. of Plasmas **19**, 056501 (2012).

[20] D. D. Ryutov *et al.*, Phys. of Plasmas **19**, 074501 (2012).

[21] C. M. Huntington *et al.*, Nat. Phys. (2015).

[22] J. R. Zhao *et al.*, Scientific Reports **6**, 27363 (2016).

[23] J. Zhao *et al.*, Rev. Sci. Inst. **86**, 063505 (2015).

[24] R. Benattar, C. Popovics, and R. Sigel, Rev. Sci. Instr. **50**, 1583 (1979).

[25] X. Liu, Y. T. Li, Y. Zhang, *et al.*, New J of Phys. **13**, 093001 (2011).

[26] S. Agostinelli, J. Allison, K. Amako, *et al.*, Nucl. Instr. & Meth. A **506**, 250 (2003).

[27] Z. S. Hartwig and P. Gumplinger, Nucl. Instr. & Meth. A **737**, 155 (2014).

[28] J. D. Moody, P. Michel, L. Divol, *et al.*, Nat Phys **8**, 344 (2012).

[29] Y. Yasutomo *et al.*, Plasma Science **9**, 18 (1981).

[30] R. Ramis, J. Meyer-ter Vehn, and J. Ramirez, Computer Physics Communications **180**, 977 (2009).

[31] C. Popovics *et al.*, Physics of Plasmas **4**, 190 (1997).

[32] T. S. Ramazanov and S. K. Kodanova, Physics of Plasmas **8**, 5049 (2001).

[33] D. D. Ryutov *et al.*, Physics of Plasmas **20**, 032703 (2013).

[34] C. K. Li, D. D. Ryutov, S. X. Hu, *et al.*, Phys. Rev. Lett. **111**, 235003 (2013).

[35] C. Bertulani, Nuclear Physics A **626**, 187 (1997).